

sMGC: A Complex-Valued Graph Convolutional Network via Magnetic Laplacian for Directed Graphs

Jie Zhang¹, Bo Hui², Po-Wei Harn², Min-Te Sun¹, Wei-Shinn Ku²

¹ National Central University, Taiwan

² Auburn University, United States

hazdzz@g.ncu.edu.tw, bohui@auburn.edu, pzh0039@auburn.edu,

msun@csie.ncu.edu.tw, weishinn@auburn.edu

Abstract

Recent advancements in Graph Neural Networks have led to state-of-the-art performance on representation learning of graphs for node classification. However, the majority of existing works process directed graphs by symmetrization, which may cause loss of directional information. In this paper, we propose the magnetic Laplacian that preserves edge directionality by encoding it into complex phase as a deformation of the combinatorial Laplacian. In addition, we design an Auto-Regressive Moving-Average (ARMA) filter that is capable of learning global features from graphs. To reduce time complexity, Taylor expansion is applied to approximate the filter. We derive complex-valued operations in graph neural network and devise a simplified Magnetic Graph Convolution network, namely sMGC. Our experiment results demonstrate that sMGC is a fast, powerful, and widely applicable GNN.

Introduction

Although Convolutional Neural Networks (CNNs) have been quite successfully applied in the computer vision domain, they are incapable of handling data embedded with graph structure, such as CoRA Sen et al. (2008) and WebKB de Campos et al. (2009). Consequently, a large number of Graph Neural Networks (GNNs) have been developed to generalize convolution operation to the graph domain. GNNs have recently been utilized in a variety of domains, such as natural language processing Beck, Haffari, and Cohn (2018), traffic prediction Yu, Yin, and Zhu (2018), social network Fan et al. (2019), and recommendation system Wang et al. (2019).

However, the graph Fourier transform Shuman et al. (2013), which is based on computing the eigendecomposition of the graph Laplacian, can not be directly used on directed graphs, since the adjacency matrix is asymmetric Stanković, Daković, and Sejdić (2019). A straightforward method is to symmetrize directed graphs into undirected graphs. Unfortunately, treating directed graphs as undirected graphs will overlook the asymmetric nature and fail to capture directional information. Another alternative solution is to utilize the theory of graph signal processing,

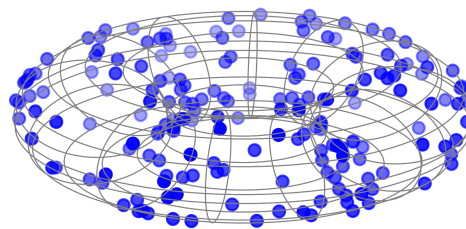


Figure 1: A schematic diagram of the magnetic eigenmap. Each node represents an eigenvector.

in which the graph Fourier transform for directed graphs is based on the Jordan decomposition of the adjacency matrix Sandryhaila and Moura (2013); Singh, Chakraborty, and Manoj (2016). There are several reasons that this method is unreliable. First, the numerical computation of the Jordan decomposition is unstable Golub and Wilkinson (1976). Second, the Fourier basis is not orthonormal, and the transform is not unitary Shafipour et al. (2018). Third, the eigenvalues of the adjacency matrix may be complex-valued Sakiyama, Namiki, and Tanaka (2017).

In this paper, we introduce the magnetic Laplacian, a novel complex-valued Hermitian matrix. It preserves edge directionality by encoding it into complex phase as an extension of the combinatorial Laplacian. The magnetic Laplacian may be regarded as a discrete Hamiltonian of a charged particle on a graph that is affected by magnetic flux Fanuel, Alaíz, and Suykens (2017). In Fanuel, Alaíz, and Suykens (2017), the magnetic Laplacian is used for community detection on directed graphs. In Furutani et al. (2019), the magnetic Laplacian is combined with GraphWave Donnat et al. (2018) for graph representation learning in directed graphs. In this research, we adopt the magnetic Laplacian for node classification in directed graphs. Figure 1 shows a schematic diagram of the magnetic eigenmap Fanuel et al. (2018), where each node represents an eigenvector which is confined in a space varying magnetic field. This explains why this Laplacian is called the magnetic Laplacian.

Graph filters extract features from graph signals. In GNNs, Finite Impulse Response (FIR) filters are widely used Zhu et al. (2021); Balcilar et al. (2021). FIR filters only aggregate finite neighborhood features of each node. Therefore, the capacity of a GNN with an FIR filter is de-

terminated by the degree k of a polynomial, which is generally an orthogonal polynomial such as Chebyshev polynomials Defferrard, Bresson, and Vandergheynst (2016). Due to this property, GNNs with an FIR filter are called k -hop GNNs. A k -hop GNN merely learns local features from a graph. Thus, the degree of the polynomial should be high enough to learn a wide range of local features. However, the computing cost increases significantly as the degree increases. In other words, a k -hop GNN would consume enormous computational resources to enhance performance. For this reason, we design an Auto-Regressive Moving-Average (ARMA) filter. First, we combine GDC (HKPR) Klicpera, Weißenberger, and Günnemann (2019) with GCN Kipf and Welling (2017) to get a smooth filter. Then, to save the computing cost, we approximate this filter with the first order Taylor series to obtain our ARMA filter. Our ARMA filter offers more smooth frequency responses than FIR filter and shows a large potential in learning global features from graphs. Note that the ARMA filters are further approximated with geometric progression in our model to reduce computational complexity.

Based on the magnetic Laplacian and ARMA filter, we design a GNN named Simplified Magnetic Graph Convolution (sMGC) network for node classification on directed graphs. Since the magnetic Laplacian is complex-valued, traditional Real-Valued Neural Network (RVNN) is not applicable anymore. To address this challenge, we design a novel complex-valued graph neural network. Specifically, we devise a complex-valued LeakyReLU and complex-valued Softmax function which are vital for node classification tasks. The magnetic Laplacian enables sMGC process directed graph in complex plane by adjusting the value of an electric charger parameter g . Our model shows the superiority over GAT Velickovic et al. (2018) and SSGC Zhu and Koniusz (2021) in terms of accuracy. All in all, our proposed sMGC is a fast, powerful, and widely applicable GNN.

We summarize the contributions of this research as follows:

1. We propose sMGC, a simplified Magnetic Graph Convolution neural network based on magnetic Laplacian to encode directional information in directed graphs.
2. We design a novel Auto-Regressive Moving Average filter to learn global features with low computational complexity.
3. We design complex-valued LeakyReLU and Softmax functions for the graph neural network to address the complex nature of magnetic Laplacian.
4. We apply our network to a variety of directed graphs and the experimental results verify the superiority of our model over existing works on node classification tasks.

Related Work

Since the emergence of Spectral CNN Bruna et al. (2014), GNNs have gained in popularity. As graph structure data are commonplace in real world, GNNs show immense potential over CNNs. This promotes GNNs to be developed as a separate branch of CNNs on graphs in recent years.

Graph Filters. Based on graph Fourier transform, Spectral CNN obtains a non-parametric filter. However, there are two shortcomings of Spectral CNN. First, the filter is not localized in vertex domain. Second, the time complexity of eigen-decomposition is $O(n^3)$, where n is the number of nodes. To address these issues, ChebyNet Defferrard, Bresson, and Vandergheynst (2016) designed a fast localized graph filter. ChebyNet is the first GNN with graph filter modification, which utilizes Chebyshev polynomials of the first kind. Then GCN Kipf and Welling (2017) improved ChebyNet by designing a linear low-pass filter based on the first order Chebyshev polynomials. It proposes a method called the renormalization trick which inspires several GNNs to design filters. As a simplified version of multi-layer GCN, SGC Wu et al. (2019) eliminates the nonlinear activation function and Dropout in order to retain performance and achieve the same results as GCN. Furthermore, to achieve great results in node classification, GraphHeat Xu et al. (2019) and GDC (HKPR) Klicpera, Weißenberger, and Günnemann (2019) choose Heat Kernel as an approach to strengthen graph filters. In addition, SSGC Zhu and Koniusz (2021) adopts Markov Diffusion Kernel to build a smooth low-pass filter. Another capacity enhancement strategy for GNNs is attention mechanism. Since the Transformer has been proposed by Google Vaswani et al. (2017), self-attention becomes increasingly popular. GAT Velickovic et al. (2018) utilizes self-attention for feature aggregating from nodes, which has become a new standard for high performance GNNs. Balcilar et al. (2021) simulates the frequency responses of GAT. The simulation results show that GAT is a low-pass filter GNN.

Heat Kernel. As a fundamental solution of the heat equation, Heat Kernel has been widely studied in graph theory Chung (1997). By associating with the Laplacian, it can be written as $e^{-t\mathbf{L}}$, where \mathbf{L} is the normalized Laplacian matrix of an undirected graph and t is a scale parameter ($t > 0$). GraphHeat adopts Heat Kernel to design a polynomial filter. As a k -hop GNN, in GraphHeat each degree of the polynomial is a smooth exponential low-pass filter. For instance, the k -degree filter is $e^{-kt\mathbf{L}}$. Based on Heat Kernel, GDC (HKPR) uses Heat Kernel PageRank Chung (2007) as a diffusion method. In these GNNs, Heat Kernel has shown its impact on enhancing the performance of GNNs.

Magnetic Laplacian. The magnetic Laplacian is first proposed in Shubin (1994). It can be considered as a discrete magnetic Schrödinger operator on graphs. The magnetic Laplacian is widely used in mathematics Colin de Verdière (2013) and physics Olgiati (2017). Since it is a complex-valued Hermitian matrix, its eigenvalues are real-valued and eigenvectors are orthonormal. Due to this property, it can be employed in graph signal processing, community detection, and GNNs for both directed and undirected graphs.

We are aware of a concurrently developed preprint work: MagNet Zhang et al. (2021), which adopts the magnetic Laplacian for node classification. This work combines the renormalization trick with the magnetic Laplacian to build a low-pass filter. Since designing a Complex-Valued Neural Network (CVNN) is challenging, they split a CVNN into two RVNNs. Specifically, MagNet separates complex-

valued tensors into the real and imaginary parts; each is processed by an independent RVNN. In the last layer, there is an unwind operation turning complex-valued tensors into real-valued tensors.

Our model is different from MagNet in several ways. First, we consider complex-valued tensors as an integration. Based on this idea, our model is a complete CVNN with corresponding complex-valued techniques such as activation function, initialization, Dropout, and Softmax. Second, we design an ARMA filter to learn global features from graphs. Moreover, to reduce time complexity, geometric progression is applied for approximation of ARMA filter in our model.

Preliminary

Directed Graphs

A directed graph G is represented as $G = \{V, E\}$, where V is the set of vertices or nodes with $|V| = n$, and $E \subseteq V \times V$ is the set of edges. Let $\mathbf{A} \in \mathbb{R}^{n \times n}$ denote the directed adjacency matrix of G , where $\mathbf{A}(u, v) = 1$ if there is an edge from node u to node v , otherwise $\mathbf{A}(u, v) = 0$.

In graph theory, directed graphs can be divided into two categories: directed acyclic graphs and directed cyclic graphs. We define a cycle in a directed graph as a closed chain of distinct edges that connects a sequence of distinct nodes. If all the edges on a cycle are oriented in the same direction, it is called a directed cycle. If a directed graph has no directed cycle, we name it a directed acyclic graph. Otherwise, the directed graph is called directed cyclic graph.

Undirected Graphs

We use $G_s = \{V, E_s\}$ to represent an undirected graph. The undirected adjacency matrix can be described by $\mathbf{A}_s = \frac{1}{2}(\mathbf{A} + \mathbf{A}^T)$. For an undirected graph, the combinatorial Laplacian can be defined as $\mathbf{L} = \mathbf{D}_s - \mathbf{A}_s$, where \mathbf{D}_s is the diagonal degree matrix. Correspondingly, its symmetric normalized form is defined as $\mathbf{L}^{sym} = \mathbf{I}_n - \mathbf{D}_s^{-\frac{1}{2}} \mathbf{A}_s \mathbf{D}_s^{-\frac{1}{2}}$, where $\mathbf{I}_n \in \mathbb{R}^{n \times n}$ is an identity matrix.

Graph Convolution

For an undirected graph G_s , its graph Laplacian can be eigendecomposed as $\mathbf{L} = \mathbf{U} \mathbf{\Lambda} \mathbf{U}^*$, where $\mathbf{U} \in \mathbb{R}^{n \times n}$ is a matrix of orthonormal eigenvectors, $\mathbf{\Lambda} = \text{diag}([\lambda^{(0)}, \dots, \lambda^{(n-1)}]) \in \mathbb{R}^{n \times n}$ is a diagonal matrix of eigenvalues, and $*$ means conjugate transpose. Since \mathbf{U} is real-valued, we have $\mathbf{U}^* = \mathbf{U}^T$.

Based on the theory of graph signal processing Shuman et al. (2013), the graph Fourier transform for a signal $x \in \mathbb{R}^n$ on the undirected graph G_s is defined as $\hat{x} = \mathbf{U}^T x$, and the inverse graph Fourier transform is $x = \mathbf{U} \hat{x}$. The convolution operator on graph $*_G$ is defined as $x *_G y = \mathbf{U} ((\mathbf{U}^T x) \odot (\mathbf{U}^T y))$, where \odot is the Hadamard product. The graph convolution formula can be rewritten as $\mathbf{U} h(\mathbf{\Lambda}) \mathbf{U}^T x$, where $h(\mathbf{\Lambda})$ is the frequency response function (FRF) of the graph filter. And the graph filter is defined as $\mathbf{U} h(\mathbf{\Lambda}) \mathbf{U}^T = h(\mathbf{U} \mathbf{\Lambda} \mathbf{U}^T) = h(\mathbf{L})$.

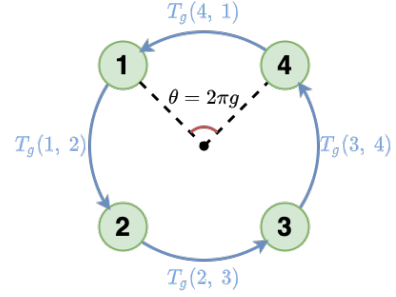


Figure 2: An illustration of a directed 4-cycle. Each arrow represents a parallel transport, and its rotation angle is θ .

Proposed Method

Magnetic Laplacian

For a directed graph, eigenvectors of the normalized Laplacian are not orthonormal Furutani et al. (2019). Thus symmetrizing \mathbf{A} into \mathbf{A}_s is a common approach Defferrard, Bresson, and Vandergheynst (2016); Kipf and Welling (2017); Xu et al. (2019). However, symmetrization will overlook the asymmetric nature and lose directional information. To address this issue, we introduce the magnetic Laplacian Fanuel, Alaíz, and Suykens (2017); Fanuel et al. (2018), which is a complex-valued Hermitian matrix. As a deformation of the combinatorial Laplacian, it is defined as:

$$\begin{aligned} \mathbf{L}_g &= \mathbf{D}_s - \mathbf{A}_s \odot \mathbf{T}_g, \\ \mathbf{T}_g(u, v) &= \exp(i2\pi g (\mathbf{A}(u, v) - \mathbf{A}(v, u))), \end{aligned} \quad (1)$$

where \mathbf{T}_g is a complex and unitary parallel transporter and $g \in [0, 0.5]$ is an electric charge parameter. We use \mathbf{T}_g to represent the direction of magnetic fluxes among nodes. For example, Figure 2 depicts a directed 4-cycle, where each circular arc with an arrowhead represents a parallel transport and θ is the rotation angle of \mathbf{T}_g . According to Fanuel, Alaíz, and Suykens (2017), g is related to directed m -cycles in a graph, where $m \in \mathbb{Z}^+$. Specifically, $g = \frac{1}{m}$ if there is a directed m -cycle ($m \geq 2$), otherwise $g = 0$. As an example, in Figure 2, $g = \frac{1}{4}$ since there is a directed 4-cycle in the graph. There are two cases that the magnetic Laplacian will be degenerated to the combinatorial Laplacian: (1) $g = 0$, (2) $\mathbf{A} = \mathbf{A}^T$. The former means the graph is a directed acyclic graph. The later means the graph is an undirected graph. The symmetric normalized magnetic Laplacian is defined as:

$$\begin{aligned} \mathbf{L}_g^{sym} &= \mathbf{D}_s^{-\frac{1}{2}} \mathbf{L}_g \mathbf{D}_s^{-\frac{1}{2}} \\ &= \mathbf{I}_n - \mathbf{D}_s^{-\frac{1}{2}} \mathbf{A}_s \mathbf{D}_s^{-\frac{1}{2}} \odot \mathbf{T}_g \end{aligned} \quad (2)$$

It has been proved by Fanuel, Alaíz, and Suykens (2017) that \mathbf{L}_g^{sym} is a positive semi-definite Hermitian matrix. Hence, eigenvectors of the \mathbf{L}_g^{sym} are orthonormal, and eigenvalues λ_g are real. More specifically, $\lambda_g \in [0, 2]$ and $0 = \lambda^{(0)} \leq \lambda_g^{(0)}$, where $\lambda^{(0)}$ represents the smallest eigenvalue of \mathbf{L}^{sym} , $\lambda_g^{(0)}$ represents the smallest eigenvalue of \mathbf{L}_g^{sym} . Then, we use the renormalization trick from GCN to get the symmetric renormalized magnetic adjacency matrix:

$$\hat{\mathbf{A}}_g = (\mathbf{D}_s + \mathbf{I}_n)^{-\frac{1}{2}} (\mathbf{A}_s + \mathbf{I}_n) (\mathbf{D}_s + \mathbf{I}_n)^{-\frac{1}{2}} \odot \mathbf{T}_g \quad (3)$$

If $g = 0$ or $\mathbf{A} = \mathbf{A}^T$, then $\hat{\mathbf{A}}_g = \hat{\mathbf{A}}$, where $\hat{\mathbf{A}} = (\mathbf{D}_s + \mathbf{I}_n)^{-\frac{1}{2}}(\mathbf{A}_s + \mathbf{I}_n)(\mathbf{D}_s + \mathbf{I}_n)^{-\frac{1}{2}}$ is used in GCN as its graph filter.

Magnetic Graph Convolution

To improve the performance of GCN, Klicpera, Weißenberger, and Günnemann (2019) utilize the diffusion method named the Heat Kernel PageRank (HKPR) to combine with GCN. Let $\tilde{\lambda} = h(\lambda)_{GCN}$ represents the FRF of GCN. Then the FRF of eigenvalues with GDC (HKPR) is defined as $h(\tilde{\lambda}) = e^{t(\tilde{\lambda}-1)}$, where $t \in \mathbb{R}^+$ represents diffusion time. To address the high time complexity of matrix exponentiation, we propose to use Taylor series as an approximation method:

$$\begin{aligned} h(\tilde{\lambda}) &= e^{t(\tilde{\lambda}-1)} = \frac{e^{\alpha t(\tilde{\lambda}-1)}}{e^{(\alpha-1)t(\tilde{\lambda}-1)}} \\ &= \frac{\sum_{k=0}^{\infty} \frac{(\alpha t(\tilde{\lambda}-1))^k}{k!}}{\sum_{k=0}^{\infty} \frac{((\alpha-1)t(\tilde{\lambda}-1))^k}{k!}} \\ &\approx \frac{1 - \alpha t(1 - \tilde{\lambda})}{1 + (1 - \alpha)t(1 - \tilde{\lambda})}, \end{aligned} \quad (4)$$

where $\alpha \in [0, 1]$. Then we have (i) when $\alpha = 0$, $h(\tilde{\lambda}) = \frac{1}{1+t(1-\tilde{\lambda})}$ and its graph filter is an impulse low-pass Auto-Regressive (AR) filter; (ii) when $\alpha = 1$, $h(\tilde{\lambda}) = 1 - t(1 - \tilde{\lambda})$ and its graph filter is a linear low-pass Moving-Average (MA) filter; (iii) when $\alpha \in (0, 1)$, $h(\tilde{\lambda}) = \frac{1 - \alpha t(1 - \tilde{\lambda})}{1 + (1 - \alpha)t(1 - \tilde{\lambda})}$ and its graph filter is an impulse low-pass Auto-Regressive-Moving-Average (ARMA) filter. Since ARMA filters are much more powerful than AR or MA filters Tremblay, Gonçalves, and Borgnat (2018), we let $\alpha \in (0, 1)$. The graph filter becomes $h(\hat{\mathbf{A}}) = \left(\mathbf{I}_n - \alpha t(\mathbf{I}_n - \hat{\mathbf{A}})\right) \left(\mathbf{I}_n + (1 - \alpha)t(\mathbf{I}_n - \hat{\mathbf{A}})\right)^{-1}$. Since $\hat{\mathbf{A}}$ is a special case of $\hat{\mathbf{A}}_g$, by replacing $\hat{\mathbf{A}}$ with our renormalized magnetic adjacency matrix $\hat{\mathbf{A}}_g$, we can get:

$$\begin{aligned} h(\hat{\mathbf{A}}_g) &= \left(\mathbf{I}_n - \alpha t(\mathbf{I}_n - \hat{\mathbf{A}}_g)\right) \left(\mathbf{I}_n + (1 - \alpha)t(\mathbf{I}_n - \hat{\mathbf{A}}_g)\right)^{-1} \\ &= \left(\frac{1 - \alpha t}{(1 - \alpha)t + 1} \mathbf{I}_n + \frac{\alpha t}{(1 - \alpha)t + 1} \hat{\mathbf{A}}_g\right) \\ &\quad \left(\mathbf{I}_n - \frac{(1 - \alpha)t}{(1 - \alpha)t + 1} \hat{\mathbf{A}}_g\right)^{-1} \end{aligned} \quad (5)$$

However, the computational cost of a matrix inversion is still huge. Inspired by Balcilar et al. (2021), the FRF of $\hat{\mathbf{A}}_g$ is defined as:

$$h(\lambda_g) \approx 1 - \frac{\bar{p}}{\bar{p} + 1} \lambda_g \quad (6)$$

Therefore, $h(\lambda_g) \in (-1, 1]$, and $\det(\hat{\mathbf{A}}_g) \leq 1$. Then we have:

$$\begin{aligned} \alpha \in (0, 1), t > 0 &\Rightarrow \frac{(1 - \alpha)t}{(1 - \alpha)t + 1} \in (0, 1) \\ \det(\hat{\mathbf{A}}_g) \leq 1 &\Rightarrow \left(\mathbf{I}_n - \frac{(1 - \alpha)t}{(1 - \alpha)t + 1} \hat{\mathbf{A}}_g\right)^{-1} \neq \mathbf{0} \end{aligned} \quad (7)$$

With these two conditions, we can use the geometric progression to approximate the matrix inversion as:

$$\left(\mathbf{I}_n - \frac{(1 - \alpha)t}{(1 - \alpha)t + 1} \hat{\mathbf{A}}_g\right)^{-1} = \sum_{j=0}^{\infty} \left(\frac{(1 - \alpha)t}{(1 - \alpha)t + 1} \hat{\mathbf{A}}_g\right)^j \quad (8)$$

Inspired by Zhou et al. (2004) and SGC Wu et al. (2019), we put Equation (8) into Equation (5), and multiply the graph filter with feature matrix in an iterative way as:

$$\begin{aligned} \bar{\mathbf{X}}^{(k)} &= \left(\frac{(1 - \alpha)t}{(1 - \alpha)t + 1} \hat{\mathbf{A}}_g\right)^k + \\ &\quad \left(\frac{1 - \alpha t}{(1 - \alpha)t + 1} \mathbf{I}_n + \frac{\alpha t}{(1 - \alpha)t + 1} \hat{\mathbf{A}}_g\right) \\ &\quad \sum_{j=0}^{k-1} \left(\frac{(1 - \alpha)t}{(1 - \alpha)t + 1} \hat{\mathbf{A}}_g\right)^j \mathbf{X}, \end{aligned} \quad (9)$$

$$\begin{aligned} \bar{\mathbf{X}}^{(K)} &= \frac{(1 - \alpha)t}{(1 - \alpha)t + 1} \hat{\mathbf{A}}_g \bar{\mathbf{X}}^{(K-1)} \\ &\quad + \left(\frac{1 - \alpha t}{(1 - \alpha)t + 1} \mathbf{I}_n + \frac{\alpha t}{(1 - \alpha)t + 1} \hat{\mathbf{A}}_g\right) \mathbf{X}, \end{aligned}$$

where $\bar{\mathbf{X}}^{(0)} = \mathbf{X} \in \mathbb{R}^{n \times n}$ is the input feature matrix, and $k \in [0, K - 2]$. As $K \rightarrow \infty$, we have $\bar{\mathbf{X}}^{(\infty)}$, which can be written as:

$$\left(\mathbf{I}_n - \alpha t(\mathbf{I}_n - \hat{\mathbf{A}}_g)\right) \left(\mathbf{I}_n + (1 - \alpha)t(\mathbf{I}_n - \hat{\mathbf{A}}_g)\right)^{-1} \mathbf{X} \quad (10)$$

Hence, we propose a GNN named Simplified Magnetic Graph Convolution (sMGC) network which is given by:

$$\hat{\mathbf{Y}} = \text{modSoftmax} \left(\bar{\mathbf{X}}^{(K)} \mathbf{W} \right) \quad (11)$$

where $\mathbf{W} \in \mathbb{R}^{n \times c}$ is a learnable weight matrix. We apply our method to node classification task and c is the number of classes. The modSoftmax is a complex-valued Softmax function for complex-valued tensors. It is defined as:

$$\begin{aligned} r &= |z| = \sqrt{\Re(z)^2 + \Im(z)^2} \\ \bar{r} &= \begin{cases} r, & \text{if } \Re(z) \geq 0, \\ -r, & \text{otherwise} \end{cases} \end{aligned} \quad (12)$$

$$\text{modSoftmax}(\bar{r}_p) = \frac{\exp(\bar{r}_p)}{\sum_q \exp(\bar{r}_q)}$$

where z represents complex-valued tensors, \Re is the real part and \Im is the imaginary part. We follow Trabelsi et al. (2018) to initialize the complex-valued weight. We remark that if $g = 0$ or $\mathbf{A} = \mathbf{A}^T$, then $\hat{\mathbf{A}}_g = \hat{\mathbf{A}} \Rightarrow h(\hat{\mathbf{A}}_g) = h(\hat{\mathbf{A}})$,

sMGC will be degenerated from CVNN to RVNN. We also propose a model named MGC for large data, which is a variant of sMGC with a complex-valued linear layer as:

$$\hat{\mathbf{Y}} = \text{modSoftmax} \left(\sigma(\bar{\mathbf{X}}^{(K)} \mathbf{W}^{(0)}) \mathbf{W}^{(1)} \right) \quad (13)$$

where σ represents a complex-valued activation function named $\mathcal{C}LeakyReLU$. As a separate activation function, it is defined as:

$$\mathcal{C}LeakyReLU(z) = LeakyReLU(\Re(z)) + iLeakyReLU(\Im(z)) \quad (14)$$

where i is the imaginary unit as $i^2 = -1$. If the imaginary part of input is $\mathbf{0}$, the $\mathcal{C}LeakyReLU$ will degenerate to real-valued LeakyReLU.

Experiments

Experiments setup

We follow the standard GNN experimental settings to evaluate sMGC and MGC on benchmark datasets for node classification. To verify the superiority of our model, we introduce GCN Kipf and Welling (2017), SGC Wu et al. (2019), gfNN NT and Maehara (2019), GraphHeat Xu et al. (2019), GDC (HKPR) Klicpera, Weißberger, and Günnemann (2019), GAT Velickovic et al. (2018), and SSGC Zhu and Koniusz (2021) as baselines. For all these baselines, we use the default setting and parameters as described in the corresponding paper. We use two types of datasets: citation network datasets and WebKB datasets. The detailed statistics of those datasets are shown in Table 1.

Citation Networks. CoRA, CiteSeer, and PubMed are standard citation network benchmark datasets Sen et al. (2008); Namata et al. (2012). In these networks, every node represents a paper and every edge represents a citation from one paper to another. The edge direction is defined from a citing paper to a cited paper. The feature is a vocabulary of unique words. We follow Yang, Cohen, and Salakhutdinov (2016) to preprocess the data into training, validation and test set.

WebKB. WebKB is a webpage dataset collected from computer science departments of various universities by Carnegie Mellon University Lu and Getoor (2003). In WebKB, there are 4 datasets named Cornell, Texas, Washington, and Wisconsin. Each node represents a webpage and each edge represents a hyperlink between two webpages. The edge direction is from the original webpage to the reference webpage. We follow previous work Pei et al. (2020) to randomly split nodes of each class into 60%, 20%, and 20% for training, validation and test set, respectively.

Hyperparameters. We train our models using an Adam optimizer and early stopping with 50 practices. We set learning rate as $1e^{-2}$, weight decay rate as $5e^{-4}$. In citation networks, $\alpha = 0.1$, $t = 10$, $K = 30$, and $g = 0$ by default. In WebKB, $\alpha = 0.9$, $t = 40$, $K = 20$, and $g = \frac{1}{3}$ by default. All experiments are compiled and tested on a Linux server equipped with an Intel i7-6700K 4.00 GHz CPU, 64 GB RAM, and an NVIDIA GeForce GTX 1080 Ti GPU.

Experiment results and analysis

In Table 2, we report the mean of classification accuracy (with standard deviation) on the test set as well as the comparison results. Our sMGC achieves state-of-the-art performance on all three citation networks. More specifically, we are able to improve upon the best baseline by a margin of 2.9% and 1.3% on CiteSeer (over GAT) and PubMed (over SSGC), respectively. The comparison results verify the advantage of the magnetic Laplacian.

For four datasets in WebKB, since the directed graph is cyclic, we have $g \neq 0$. More specifically, $g = \frac{1}{3}$ since a directed 3-cycle exists in Cornell, Texas, Washington, and Wisconsin. We observe that GNNs without Heat Kernel are over-fitting in WebKB. This phenomenon shows Heat Kernel has a great potential in graph learning. Due to our $\mathcal{C}LeakyReLU$, MGC performs better than sMGC in WebKB.

In Figure 3, we depict FRFs of all baseline models and our methods. For GCN, its frequency responses rely on average node degree of graphs due to the renormalization trick. The result on all three datasets show that GCN has a linear low-pass filter, and its filter does not cover the whole spectrum. Therefore, GCN cannot learn features of the whole graph. We can consider SGC as a multi-layer GCN, thus SGC also works as a low-pass filter GNN. From the result on all three datasets, we find that SGC focuses more on high frequency, which is different from other GNNs. That is the reason why the experiment results of SGC are not good enough. The baseline gfNN equals to SGC plus a linear layer. Therefore, gfNN has the same filter as SGC. As a result, the classification performances of gfNN on citation networks are almost the same as SGC’s. As a k -hop GNN with Heat Kernel polynomials, GraphHeat’s FRF is smoother than the others. Due to this property, its FRF is close to 0 in high frequency. Thus, GraphHeat cannot learn high frequency information in graphs. GCN with GDC (HKPR) has the same problem. When comparing SSGC with sMGC, we find that the FRFs of SSGC are lower than sMGC’s in low frequency. Therefore, SSGC learns fewer features in graphs than sMGC. sMGC and MGC both have a low-pass filter.

The FRFs of sMGC and MGC are the same in CoRA, sMGC learns more low frequency than MGC in CiteSeer, and MGC learns less high frequency information than sMGC in PubMed. We have not drawn the FRFs of ChebyNet because its frequency responses do not change for different graphs Balcilar et al. (2021). The filter of ChebyNet is complicated. Each term of Chebyshev Polynomials of the first kind has a different filter. For the first term, it is an all-pass filter. For the second term, it is a high-pass filter. For k^{th} term ($k \geq 3$), it is a comb filter which is a combination of low-pass and high-pass filters Balcilar et al. (2021). This property leads ChebyNet to focus more on local features than global ones. GAT is based on attention mechanism and we are not able draw its FRFs directly. We follow Balcilar et al. (2021) to simulate its FRFs. The simulation results show that GAT is a low-pass filter GNN, and it has wide fluctuations of frequency responses in CoRA. This implies that GAT is unstable in learning graph features.

Table 1: Statistics of datasets

| | CoRA | CiteSeer | PubMed | Cornell | Texas | Washington | Wisconsin |
|-----------|------|----------|--------|---------|-------|------------|-----------|
| #Nodes | 2708 | 3327 | 19717 | 195 | 187 | 230 | 265 |
| #Edges | 5429 | 4732 | 44338 | 304 | 328 | 446 | 530 |
| #Features | 1433 | 3703 | 500 | 1703 | 1703 | 1703 | 1703 |
| #Classes | 7 | 6 | 3 | 5 | 5 | 5 | 5 |

Table 2: Performance comparison

| Model | CoRA | CiteSeer | PubMed | Cornell | Texas | Washington | Wisconsin |
|------------|---------------------|---------------------|---------------------|---------------------|--------------|--------------|---------------------|
| ChebyNet | 79.95 ± 0.75 | 70.35 ± 0.85 | 71.35 ± 0.25 | 74.36 ± 2.56 | 68.42 ± 2.63 | 70.66 ± 1.08 | 82.08 ± 2.83 |
| GCN | 80.65 ± 0.45 | 69.25 ± 0.55 | 77.00 ± 0.50 | 44.87 ± 1.28 | 55.26 ± 0.00 | 63.05 ± 2.17 | 59.44 ± 0.94 |
| SGC | 80.40 ± 0.00 | 68.80 ± 0.10 | 76.95 ± 0.05 | 41.03 ± 0.00 | 55.26 ± 0.00 | 60.87 ± 0.00 | 58.49 ± 0.00 |
| gfNN | 79.35 ± 0.45 | 65.05 ± 0.15 | 76.50 ± 0.20 | 42.31 ± 1.28 | 57.89 ± 0.00 | 63.05 ± 2.17 | 55.66 ± 0.94 |
| GraphHeat | 81.30 ± 1.10 | 69.25 ± 0.15 | 76.00 ± 0.80 | 75.64 ± 3.85 | 82.90 ± 1.31 | 69.57 ± 2.17 | 82.08 ± 0.94 |
| GDC (HKPR) | 80.55 ± 0.45 | 69.70 ± 0.40 | 77.30 ± 0.30 | 76.92 ± 0.00 | 77.64 ± 1.31 | 70.66 ± 1.08 | 83.97 ± 0.94 |
| GAT | 82.60 ± 0.40 | 70.45 ± 0.25 | 77.45 ± 0.45 | 41.03 ± 0.00 | 52.63 ± 2.63 | 63.04 ± 0.00 | 56.61 ± 1.88 |
| SSGC | 80.20 ± 0.00 | 67.95 ± 0.65 | 78.65 ± 0.05 | 69.23 ± 0.00 | 68.42 ± 0.00 | 67.39 ± 0.00 | 81.13 ± 0.00 |
| sMGC | 82.70 ± 0.00 | 73.30 ± 0.00 | 79.90 ± 0.10 | 73.08 ± 1.28 | 71.05 ± 0.00 | 68.48 ± 3.26 | 80.19 ± 2.83 |
| MGC | 82.50 ± 1.00 | 71.25 ± 0.95 | 79.70 ± 0.40 | 80.77 ± 3.85 | 82.90 ± 1.31 | 70.66 ± 1.08 | 87.74 ± 2.83 |

Table 3: Ablation experiments

| dataset | sMGC | | MGC | |
|------------|---------|------------|---------|------------|
| | $g = 0$ | $g \neq 0$ | $g = 0$ | $g \neq 0$ |
| Cornell | 66.67 | 74.31 | 69.23 | 84.62 |
| Texas | 78.94 | 71.05 | 71.05 | 84.31 |
| Washington | 67.39 | 71.74 | 65.22 | 71.74 |
| Wisconsin | 69.81 | 83.02 | 77.36 | 90.57 |

Table 4: Running time (seconds) per epoch

| Model | CoRA | CiteSeer | PubMed |
|------------|---------------|---------------|---------------|
| ChebyNet | 0.1660 | 0.5298 | 3.2450 |
| GCN | 0.0179 | 0.0316 | 0.6184 |
| SGC | 0.0028 | 0.0065 | 0.0055 |
| gfNN | 0.0049 | 0.0128 | 0.0147 |
| GraphHeat | 0.1390 | 0.4861 | 2.9142 |
| GDC (HKPR) | 0.0178 | 0.0315 | 0.6206 |
| GAT | 0.4753 | 1.0237 | 19.4280 |
| SSGC | 0.0036 | 0.0080 | 0.0071 |
| sMGC | 0.0027 | 0.0062 | 0.0055 |
| MGC | 0.0053 | 0.0130 | 0.0185 |

Ablation study

Note that datasets in WebKB can be represented as directed cyclic graphs, thus $g \neq 0$. In order to study how the electric changer parameter g affects the performance of sMGC and MGC, more specifically in order to assess the benefit of the edge direction, we compare $g = 0$ and $g \neq 0$. Recall when $g = 0$, sMGC and MGC would be degenerated from CVNN to RVNN; thus the ablation experiment results also show the comparison between CVNN and RVNN. As shown in Table 3, when the value of $g \neq 0$, which means the model is CVNN, sMGC and MGC have better experiment results. It verifies the effectiveness of CVNN and the magnetic Lapla-

cian on directed cyclic graphs.

Running time analysis

To verify the efficiency of our model, we compare the training time of each epoch with these baseline models. As shown in Table 4, the training time (each epoch) of our sMGC is least on CoRA, CiteSeer, and PubMed. More specifically, the training time of our sMGC is less than 0.5% of GAT and the same as that of SGC and SSGC. This is because sMGC and SSGC follow SGC which multiplies the graph filter with input features first. It causes the graph convolution to be simplified as a linear layer.

We also investigate the efficiency of our approximation method. Table 5 provides the time complexity of calculating filter for the original method and different approximation. Compared with the original GDC (HKPR), the first approximation (notation as $K = 0$) can reduce the calculation time significantly. The second approximation ($K \neq 0$) can further reduce the calculation time. As the value of K decreases, the running time of second approximation also decreases. We remark that our approximation is especially useful on large graphs. For example, on PubMed, the calculation time of GDC (HKPR) is 783 seconds (13 minutes), where it only takes 9.14 seconds (1% of GDC (HKPR)) with our approximation ($K = 30$).

Discussion

There are two definitions of the magnetic Laplacian, differing by a minus sign. In Fanuel, Alafz, and Suykens (2017), $\mathbf{L}_g = \mathbf{D}_s - \mathbf{A}_s \odot \mathbf{T}_g$, where $\mathbf{T}_g(u, v) = \exp(i2\pi g(\mathbf{A}(v, u) - \mathbf{A}(u, v)))$. In Fanuel et al. (2018), $\mathbf{L}_g = \mathbf{D}_s - \mathbf{A}_s \odot \mathbf{T}_g$, where $\mathbf{T}_g(u, v) = \exp(i2\pi g(\mathbf{A}(u, v) - \mathbf{A}(v, u)))$. In this paper, we choose the definition of the latter. The former magnetic Laplacian is the Hermitian transpose of the latter. Thus, both magnetic Laplacians have the same eigenvalues. Therefore, if a GNN

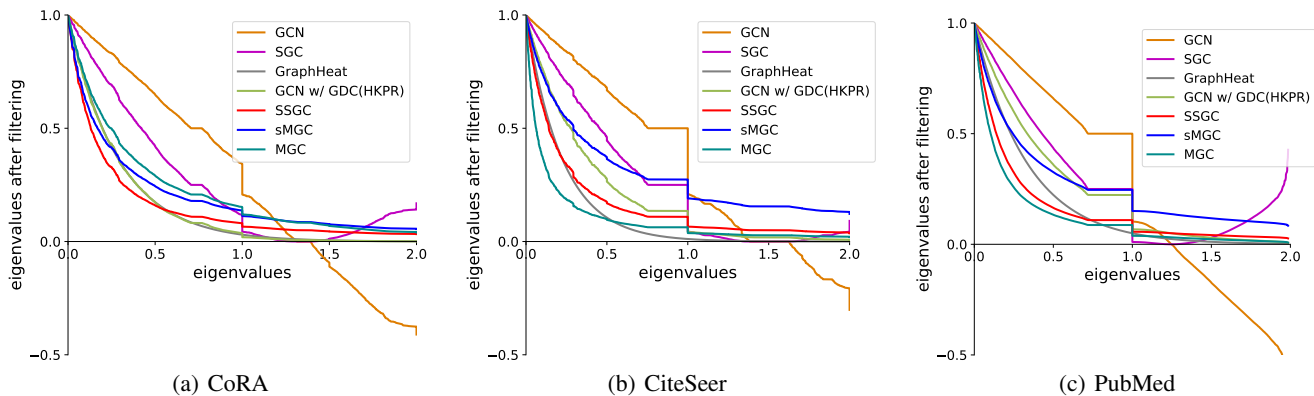


Figure 3: FRF of different methods

Table 5: Calculation time (seconds) w.r.t. Approximation

| Dataset | GDC (HKPR) | K=0 | K=5 | K=10 | K=15 | K=20 | K=25 | K=30 | K=35 | K=40 |
|----------|------------|--------|------|------|------|------|------|------|-------|-------|
| CoRA | 2.86 | 1.88 | 0.13 | 0.42 | 0.74 | 1.06 | 1.37 | 1.67 | 1.98 | 2.30 |
| CiteSeer | 4.51 | 2.14 | 0.20 | 0.69 | 1.38 | 2.10 | 2.80 | 3.45 | 4.13 | 4.81 |
| PubMed | 783.21 | 283.87 | 1.17 | 2.75 | 4.34 | 5.95 | 7.52 | 9.14 | 10.75 | 12.35 |

uses the magnetic Laplacian, adopting either definition has no influence on the performance of the GNN.

We notice that some of state-of-the-art GNNs are mini-batch based models. This approach speeds up the training process and allows GNNs to be applied for super-secrecy data. However, determining the value of electric charge parameter g in each batch is a challenging issue because the value of g depends on the existence of the directed m -cycle. If the mini-batch method is based on graph partition, how to partition graphs will directly influence the directed m -cycle. If partitioned inappropriately, each sub-graph may become directed acyclic graph. In this situation, the value of g for each batch is 0, which will cause the model to lose the advantage of the magnetic Laplacian. In addition, if the majority of sub-graphs are directed cyclic graphs, and others are directed acyclic graphs, how to decide the value of g for each batch is also an issue. In the future, we will further optimize the network structure and explore the possibility of different kinds of mini-batch training methods for our models.

Visualization

We introduce t-SNE van der Maaten and Hinton (2008), which computes the 2D coordinates from the output of CoRA (classification probabilities), to visualize nodes in a 2-dimensional space. Note that there are 7 classes on CoRA. As shown in Figure 4(a), each color represents one of 7 classes. We can see that visualization of nodes exhibits discernible clustering in the projected 2D space and these clusters correspond to 7 labels of CoRA. We also compute the 3D t-SNE coordinates and visualize these nodes in a 3-dimensional space. As shown in Figure 4(b), nodes with the same label are clustered in the 3-D space. It verifies that our model is powerful to discriminate different classes.

Conclusion

In this paper, we propose sMGC, a magnetic Laplacian based graph convolutional network to address edge directionality ignored by most existing GNN models. Specifically, our model preserves edge direction information by encoding it into complex phase as a deformation of the combinatorial Laplacian. We also design an ARMA filter to learn global features from graphs with affordable cost. We further reduce time complexity by using Taylor expansion to approximate the filter. The experiment results show that our sMGC is a fast, powerful, and widely applicable GNN.

References

- Balcilar, M.; Renton, G.; Héroux, P.; Gaüzère, B.; Adam, S.; and Honeine, P. 2021. Analyzing the Expressive Power of Graph Neural Networks in a Spectral Perspective. In *ICLR 2021*.
- Beck, D.; Haffari, G.; and Cohn, T. 2018. Graph-to-Sequence Learning using Gated Graph Neural Networks. In *ACL 2018*, 273–283.
- Bruna, J.; Zaremba, W.; Szlam, A.; and LeCun, Y. 2014. Spectral Networks and Locally Connected Networks on Graphs. In Bengio, Y.; and LeCun, Y., eds., *ICLR 2014*.
- Chung, F. 2007. The heat kernel as the pagerank of a graph. *Proceedings of the National Academy of Sciences*, 104(50): 19735–19740.
- Chung, F. R. K. 1997. *Spectral Graph Theory*. 92. American Mathematical Society.
- Colin de Verdière, Y. 2013. Magnetic interpretation of the nodal defect on graphs. *Analysis & PDE*, 6(5): 1235–1242.
- de Campos, L. M.; Fernández-Luna, J. M.; Huete, J. F.; Masegosa, A. R.; and Romero, A. E. 2009. Link-Based

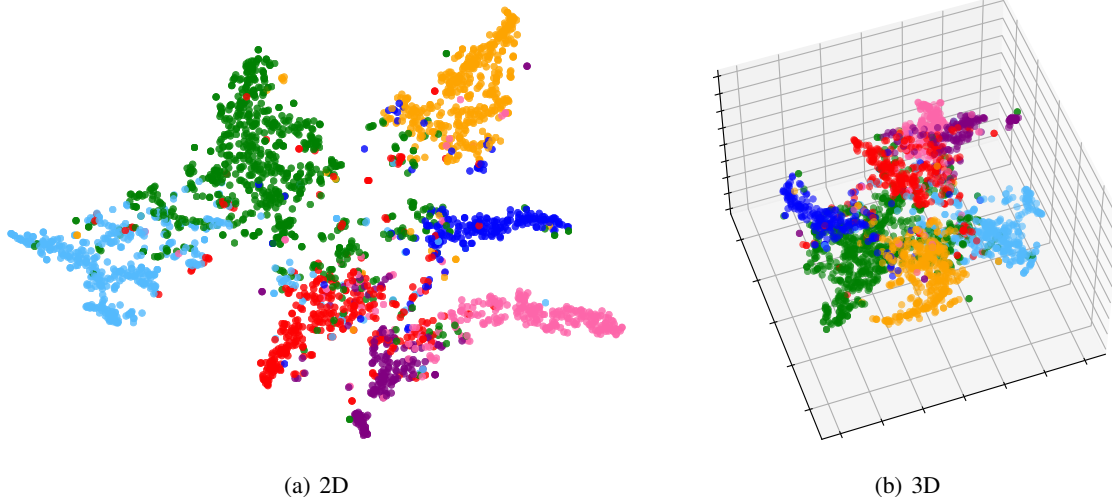


Figure 4: Visualization of nodes in CoRA (different colors represent different labels)

- Text Classification Using Bayesian Networks. In Geva, S.; Kamps, J.; and Trotman, A., eds., *INEX 2009*, volume 6203 of *Lecture Notes in Computer Science*, 397–406.
- Defferrard, M.; Bresson, X.; and Vandergheynst, P. 2016. Convolutional Neural Networks on Graphs with Fast Localized Spectral Filtering. In Lee, D. D.; Sugiyama, M.; von Luxburg, U.; Guyon, I.; and Garnett, R., eds., *Nips 2016*, 3837–3845.
- Donnat, C.; Zitnik, M.; Hallac, D.; and Leskovec, J. 2018. Learning Structural Node Embeddings via Diffusion Wavelets. In Guo, Y.; and Farooq, F., eds., *KDD 2018*, 1320–1329.
- Fan, W.; Ma, Y.; Li, Q.; He, Y.; Zhao, Y. E.; Tang, J.; and Yin, D. 2019. Graph Neural Networks for Social Recommendation. In *WWW 2019*, 417–426.
- Fanuel, M.; Alaíz, C. M.; Fernández, Á.; and Suykens, J. A. 2018. Magnetic Eigenmaps for the visualization of directed networks. *Applied and Computational Harmonic Analysis*, 44(1): 189–199.
- Fanuel, M.; Alaíz, C. M.; and Suykens, J. 2017. Magnetic eigenmaps for community detection in directed networks. *Physical review. E*, 95 2-1: 022302.
- Furutani, S.; Shibahara, T.; Akiyama, M.; Hato, K.; and Aida, M. 2019. Graph Signal Processing for Directed Graphs Based on the Hermitian Laplacian. In *PKDD 2019*, volume 11906 of *Lecture Notes in Computer Science*, 447–463.
- Golub, G. H.; and Wilkinson, J. H. 1976. Ill-Conditioned Eigensystems and the Computation of the Jordan Canonical Form. *SIAM Review*, 18(4): 578–619.
- Kipf, T. N.; and Welling, M. 2017. Semi-Supervised Classification with Graph Convolutional Networks. In *ICLR 2017*.
- Klicpera, J.; Weißenberger, S.; and Günnemann, S. 2019. Diffusion Improves Graph Learning. In *NeurIPS 2019*, 13333–13345.
- Lu, Q.; and Getoor, L. 2003. Link-based Classification. In Fawcett, T.; and Mishra, N., eds., *ICML 2003*, 496–503.
- Namata, G. M.; London, B.; Getoor, L.; and Huang, B. 2012. Query-driven Active Surveying for Collective Classification. In *Workshop on Mining and Learning with Graphs*.
- NT, H.; and Maehara, T. 2019. Revisiting Graph Neural Networks: All We Have is Low-Pass Filters. *CoRR*, abs/1905.09550.
- Olgiati, A. 2017. *Remarks on the Derivation of Gross-Pitaevskii Equation with Magnetic Laplacian*, 257–266. Cham: Springer International Publishing.
- Pei, H.; Wei, B.; Chang, K. C.; Lei, Y.; and Yang, B. 2020. Geom-GCN: Geometric Graph Convolutional Networks. In *ICLR 2020*.
- Sakiyama, A.; Namiki, T.; and Tanaka, Y. 2017. Design of polynomial approximated filters for signals on directed graphs. In *2017 IEEE Global Conference on Signal and Information Processing (GlobalSIP)*, 633–637.
- Sandryhaila, A.; and Moura, J. M. F. 2013. Discrete Signal Processing on Graphs. *IEEE Transactions on Signal Processing*, 61(7): 1644–1656.
- Sen, P.; Namata, G.; Bilgic, M.; Getoor, L.; Gallagher, B.; and Eliassi-Rad, T. 2008. Collective Classification in Network Data. *AI Mag.*, 29(3): 93–106.
- Shafipour, R.; Khodabakhsh, A.; Mateos, G.; and Nikolova, E. 2018. Digraph Fourier Transform via Spectral Dispersion Minimization. In *2018 (ICASSP)*, 6284–6288.
- Shubin, M. A. 1994. Discrete magnetic Laplacian. *Communications in Mathematical Physics*, 164(2): 259 – 275.
- Shuman, D. I.; Narang, S. K.; Frossard, P.; Ortega, A.; and Vandergheynst, P. 2013. The Emerging Field of Signal Processing on Graphs: Extending High-Dimensional Data Analysis to Networks and Other Irregular Domains. *IEEE Signal Process. Mag.*, 30(3): 83–98.

- Singh, R.; Chakraborty, A.; and Manoj, B. S. 2016. Graph Fourier transform based on directed Laplacian. In *2016 International Conference on Signal Processing and Communications (SPCOM)*, 1–5.
- Stanković, L.; Daković, M.; and Sejdić, E. 2019. *Introduction to Graph Signal Processing*, 3–108. Cham: Springer International Publishing.
- Trabelsi, C.; Bilaniuk, O.; Zhang, Y.; Serdyuk, D.; Subramanian, S.; Santos, J. F.; Mehri, S.; Rostamzadeh, N.; Bengio, Y.; and Pal, C. J. 2018. Deep Complex Networks. In *ICLR 2018*.
- Tremblay, N.; Gonçalves, P.; and Borgnat, P. 2018. Design of graph filters and filterbanks. In Djurić, P. M.; and Richard, C., eds., *Cooperative and Graph Signal Processing*, 299–324. Academic Press.
- van der Maaten, L.; and Hinton, G. 2008. Visualizing Data using t-SNE. *Journal of Machine Learning Research*, 2579–2605.
- Vaswani, A.; Shazeer, N.; Parmar, N.; Uszkoreit, J.; Jones, L.; Gomez, A. N.; Kaiser, L.; and Polosukhin, I. 2017. Attention is All you Need. In *Nips 2017, Long Beach, CA, USA*, 5998–6008.
- Velickovic, P.; Cucurull, G.; Casanova, A.; Romero, A.; Liò, P.; and Bengio, Y. 2018. Graph Attention Networks. In *ICLR 2018*. OpenReview.net.
- Wang, H.; Zhang, F.; Zhang, M.; Leskovec, J.; Zhao, M.; Li, W.; and Wang, Z. 2019. Knowledge-aware Graph Neural Networks with Label Smoothness Regularization for Recommender Systems. In *KDD 2019*, 968–977. ACM.
- Wu, F.; Jr., A. H. S.; Zhang, T.; Fifty, C.; Yu, T.; and Weinberger, K. Q. 2019. Simplifying Graph Convolutional Networks. In Chaudhuri, K.; and Salakhutdinov, R., eds., *ICML 2019*, volume 97 of *Proceedings of Machine Learning Research*, 6861–6871.
- Xu, B.; Shen, H.; Cao, Q.; Cen, K.; and Cheng, X. 2019. Graph Convolutional Networks using Heat Kernel for Semi-supervised Learning. In Kraus, S., ed., *IJCAI 2019*, 1928–1934.
- Yang, Z.; Cohen, W. W.; and Salakhutdinov, R. 2016. Revisiting Semi-Supervised Learning with Graph Embeddings. In Balcan, M.; and Weinberger, K. Q., eds., *ICML 2016*, 40–48.
- Yu, B.; Yin, H.; and Zhu, Z. 2018. Spatio-Temporal Graph Convolutional Networks: A Deep Learning Framework for Traffic Forecasting. In Lang, J., ed., *IJCAI 2018*, 3634–3640.
- Zhang, X.; He, Y.; Brugnone, N.; Perlmutter, M.; and Hirn, M. J. 2021. MagNet: A Magnetic Neural Network for Directed Graphs. *CoRR*, abs/2102.11391.
- Zhou, D.; Bousquet, O.; Lal, T.; Weston, J.; and Schölkopf, B. 2004. Learning with Local and Global Consistency. In Thrun, S.; Saul, L.; and Schölkopf, B., eds., *Advances in Neural Information Processing Systems*, volume 16. MIT Press.
- Zhu, H.; and Koniusz, P. 2021. Simple Spectral Graph Convolution. In *ICLR*.
- Zhu, M.; Wang, X.; Shi, C.; Ji, H.; and Cui, P. 2021. Interpreting and Unifying Graph Neural Networks with An Optimization Framework. In *WWW 2021*, 1215–1226.